Journal of the Nigerian Mathematical Society
Vol. 38, Issue 1, pp. 89-121, 2019

MHD BOUNDARY LAYER FLOW PAST A MOVING PLATE WITH MASS TRANSFER AND BINARY CHEMICAL REACTION

A. M. OKEDOYE[1] AND P. O. OGUNNIYI

ABSTRACT. In this paper the study of heat and mass transfer in unsteady natural convection MHD boundary layer flow past a moving plate with binary chemical reaction is investigated analytically. The fluid limiting surface is moved impulsively, with a constant velocity, either in the direction of the flow or in the opposite direction, in the presence of a transverse magnetic field. Both frequency-dependent effects and "long-time" effects that would require non-practically long channels to be observed in steady flow was also studied. A mathematical exploration is made into important aspects of reaction engineering in reactive flow, especially residence time flow behaviour, scale-up and scale-down procedures. From the present study it is observed amongst others that temperature increases as the fluid angular velocity increases, maximum temperatures exist in the body of the fluid, concentration increases with an increase in generative chemical reaction and vice-versa and concentration phase decreases with increase in generative chemical reaction. Also, mean velocity was seen to decrease with increase in generative chemical reaction and reaction order, and increases when the limiting surface moves in the positive direction of the flow. The graphical representation of governing flow parameters were presented and discussed. Flow conditions at the wall were also investigated, presented and discussed.

Keywords and phrases: Oscillatory; Magnetohydrodynamic; mass transfer; Permeable surface; Porous medium

2010 Mathematical Subject Classification: 76W05

1. INTRODUCTION

Many chemically reacting systems involve the species chemical reactions with finite Arrhenius activation energy, with examples

Received by the editors April 06, 2018; Revised March 12, 2019 ; Accepted: March 12, 2019

www.nigerianmathematicalsociety.org; Journal available online at https://ojs.ictp.it/jnms/

[1]Corresponding author

occurring in geothermal and oil reservoir engineering. The interactions between mass transport and chemical reactions are generally very complex, and can be observed in the production and consumption of reactant species at different rates both within the fluid and the mass transfer. Mixed convection problem along an isothermal vertical porous medium with injection and suction was reported by Hooper et al. [1]. Singh et al. [2] studied heat and mass transfer in MHD flow of a viscous fluid past a vertical porous plate under oscillatory suction velocity. Mixed convection magnetohydrodynamics flow past an infinite vertical porous plate with variable suction and oscillating plate temperature as well as flow past an infinite vertical plate with constant suction were reported in the work Sharma et al. [3]-[5]. Aaiza et al [6] investigated phenomenon of energy transfer in mixed convection unsteady MHD flow of an incompressible nanofluid inside a channel filled with saturated porous medium. is investigated. Viscosity and thermal conductivity are reported to be the most prominent parameters responsible for different results of velocity and temperature. Sharma , Chand, Chaudhary [7] obtained approximate solution of unsteady mixed convection flow of an electrically conducting fluid past an infinite vertical porous plate immersed in porous medium with constant transverse magnetic. Various governing parameters such as amplitude and phase of the skin-friction and the rate of heat transfer were discussed. The flow of Heat transfer in mixed convection inside a square cavity was reported by Sebdani et al. [8] and in a horizontal channel filled with nanofluids was reported by Fan et al. [9]. While Tiwari and Das [10] and Sheikhzadeh et al. [11] presented an analysis of laminar mixed convection flow of a nanofluid in two-sided lid-driven enclosures. A locally similarity solution of unsteady natural convection heat and mass transfer boundary layer flow past a flat porous plate and the effects of chemical reaction rate which is function of temperature and Arrhenius activation energy on the velocity, temperature and concentration were reported by Maleque [[12], [13]]. Also, Okedoye [[14], [15]] investigated and report on the Unsteady MHD mixed convection flow past an oscillating plate with heat source/sink. Makinde and Animasaun [16] investigated the effect of magnetic field, nonlinear thermal radiation and homogeneous-heterogeneous quartic autocatalysis chemical reaction on an electrically conducting alumina-water nanofluid containing gyrotactic-microorganism over an upper horizontal surface of a paraboloid of revolution. They assumed that viscosity and thermal conductivity

vary with volume fraction and adopted a suitable models. Their findings reveal that for any values of magnetic field parameter, the local skin friction coefficient is larger at high values of thickness parameter while local heat transfer rate is smaller at high values of temperature parameter.

A chemically reacting flow is a fluid flow in which a chemical reaction is also occurring. Such flows occur in a wide range of fields including combustion, chemical engineering, biology, and pollution abatement. For most liquids, the viscosity decreases with temperature and increases with pressure. For gases, it increases with both temperature and pressure. In general, the higher the viscosity of a substance, the more resistance it presents to flow (and hence more difficult to pump!). Chemical reaction can be explained as an interaction between two or more chemicals which produces either one or more new chemical compounds. Many chemical reactions actually require heat and accelerator. A chemical reaction in which catalyst is in the same phase (i.e. in the same state of matter) as the reactant(s) is/are known as homogeneous catalytic reaction. Reactions between two gases, between two liquids and mixture of household cooking gas with oxygen gas leading to flame are typical examples of homogeneous catalytic reactions [17]. When fluid moves along a surface, a thin layer is formed in the vicinity of a surface bounding the fluid; Ludwig Prandtl called it "boundary layer". Mass transfer process with chemical reaction has been given special attention in the past ([18]-[23] and ref. there in) because of its significance in chemical engineering, geothermal reservoirs, nuclear reactor cooling and thermal oil recovery. Bestman [24]was probably the first to study the boundary layer flow involving the binary chemical reaction. He analytically examined the effects of the activation energy on natural convection flow in a porous medium by using perturbation approach. One of the factors that have an important role in chemical reaction is the activation energy. It is defined as the least obligatory amount of energy for atoms or molecules to bring themselves in a state in which they can undergo a chemical reaction. The concept of activation energy is usually applicable in areas pertaining to geothermal or oil reservoir engineering and mechanics of water and oil emulsions. Activation energy can be realized as energy barrier that separates two minima of potential energy (of the reactants and products of a reaction) which has to be overcome by reactants to initiate a chemical reaction. Makinde et al. citej25

presented the numerical solution for unsteady convection flow over a flat porous plate with nth order chemical reaction and Arrhenius activation energy. The recent attempts in this direction were made by Maleque [26]-[27] who investigated the influence of binary chemical reaction with Arrhenius activation energy on mixed convection flows. Abbas et.al [28] in their work on the heat and mass transfer analysis in an unsteady boundary layer flow of a Casson fluid near a stagnation point over a stretching/shrinking sheet in the presence of thermal radiation. They considered the effects of binary chemical reaction with Arrhenius activation energy by taking chemical reaction rate as the function of temperature. Other relevant work on fluid flow with chemical reaction could be found in the work of Resbois and Leener [29] and Van der Hoek [30]. Salawu and Okedoye [31] examined the second law of thermodynamic gravity-driven viscous combustible fluid flow of two step exothermic chemical reaction with heat absorption and convective cooling under bimolecular kinetic. The important of two-steps chemical reaction in combustion processes cannot be over emphasis due to it support in complete combustion of unburned ethanol [32]. This assists in lowering the release into the atmosphere the toxic air pollutant that degrade the environment. Makinde et al. [33] studied the thermal stability of two-step exothermic chemical reaction in a slab. In the work of Makinde and Animasaum [16], the combined effects of buoyancy force, Brownian motion, thermophoresis and quartic autocatalytic chemical reaction on bioconvection of nanofluid containing gyrotactic microorganism over an upper horizontal surface of a paraboloid of revolution were presented. They assumed that the thermo-physical of the nanofluid does not vary with volume fraction. It was reported that Brownian motion boosts concentration of bulk fluid while thermophoresis reduces it. Mass transfer has relevance in most living-matter processes such as respiration, nutrition, sweating etc. The heat/mass transfer effects on revolving flow of Maxwell fluid due to unidirectional stretching surface. Mass transfer process is modeled in terms of binary chemical reaction and activation energy by invoking modified Arrhenius function for activation energy was reported by Shafique et al. [34]. Makinde and Olanrewaju [35] provided a numerical solution to the unsteady mixed convection with Dufour and Soret effects past a semi-infinite vertical porous flat plate moving through a binary mixture of chemically reacting fluid. Other contributions in this area include those of Abdul Maleque [[36]– [38]], who investigated the effects of chemical

reactions with Arrhenius activation Energy on unsteady convection heat and mass transfer boundary layer fluid flow.

The applications of Magnetohydrodynamic flow and heat transfer in engineering and technology was found in area such as MHD generators, plasma studies, nuclear reactors and geothermal energy extractions. Many researchers reported their findings in the area of Magnetohydrodynamic flow and heat transfer, Buoyancy induced flows, and flows in rotating fluids. Some of the earliest studies on the aforementioned areas could be found in the work of Soundalgekar et al. [39], who investigated the unsteady rotating flow of incompressible, viscous fluid past an infinite porous plate and Bergstrom [40] who reported boundary layer flow problem formed in a rotating fluid by oscillating flow over an infinite half-plate. Other earlier works include Nazar et al. [41], Abbas et al. [42], Zheng et al. [43], Makinde et.al [44], Makinde and Olanrewaju [45] and Chamkha et.al[46]. Okedoye and Ayandokun [47] investigated the entropy generation in MHD heat and Hall Effect of an oscillating plate in a Porous medium. In the work of Shafique et.al [48], the heat/mass transfer effects on revolving flow of Maxwell fluid due to unidirectional stretching surface was investigated where they reported that the solute concentration in binary mixture is proportional to both rotation parameter k and activation energy E, the reaction rate r and fitted rate n both provide reduction in the solute concentration. The problem of unsteady convection with chemical reaction and radiative heat transfer past a flat porous plate moving through a binary mixture in an optically thin environment investigated by Makinde et al. [49]. Makinde [50] explored the influence of melting, heat transfer and thermal stratification by modifying classical boundary condition of temperature in the Heat Transfer and Lorentz Force Effects on the Flow of MHD Casson Fluid over an Upper Horizontal Surface of a Thermally Stratified Melting Surface of a Paraboloid of Revolution. The significance of Lorentz force on the boundary layer flow of Casson fluid over an upper horizontal surface of a thermally stratified melting surface of a paraboloid of revolution provide explanation on the motion of Casson fluid over an upper horizontal surface of a thermally stratified melting surface of a paraboloid of revolution. The importance of geometry in heat and mass transfer processes of many engineering and industrial applications is buttressed by the work of

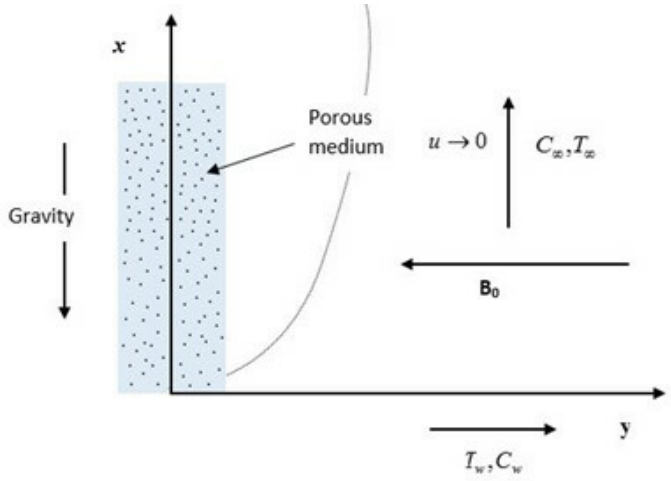

FIGURE 1. Flow geometry

Makinde et al. [51]. The thermal boundary layer of Cattaneo-Christov heat flux, external magnetic field chemical reaction, heat source and buoyant forces was found to be highly effective on the flow over a wedge when compared with plate and cone. Avinash et al. [52] investigated gyrostatic microorganisms contained MHD flow over a vertical plate. Their results reveal that increases in thermophoresis and Brownian motion brings about increase in the heat transfer rate of motile microorganisms. Despite the effort of the previous researchers chemically reacting flow, there is emerging needs for determination of the unsteady natural convection MHD boundary layer flow past a moving Plate with Mass Transfer and a Binary Chemical Reaction.

2. FORMULATION OF THE PROBLEM

Unsteady, free convection flow of an incompressible and electrically conducting viscous fluid along an infinite non conducting vertical flat plate through a porous medium with velocity components (u, v) in the (x, y) direction was considered. The limiting surface is moved impulsively, with a constant velocity, either in the direction of the flow or in the opposite direction in the presence of transverse magnetic field. In Cartesian co – ordinate system, x-axis is assumed to be along the plate in the direction of the flow and y – axis normal to it. A magnetic field of uniform strength B_0 is applied in the direction of flow and the temperature field is neglected. Initially, the plate and the fluid are at same temperature T_w in a stationary

condition with concentration level C_w at all points. At time $t > 0$ the plate starts oscillating in its own plane with a velocity U_0. Its temperature is raised to T_w and the concentration level at the plate is raised to C_w. The ambient condition is given by ϕ_∞ (where $\phi = \{u, T, C\}$) and the part associated with motion called, dynamic part ϕ_d is given as $\phi_d = \phi - \phi_\infty$. The suffix $_\infty$ in the derivatives is omitted since it is a constant. The binary chemical reaction follows the one used by Boddington, Feng and Gray [53], and Ogunseye and Okoya [54]. The equations - continuity, fluid momentum, energy and species equations in the neighborhood of the plate governing the motion is described by the following respectively;

$$\frac{\partial v}{\partial y} = 0, \tag{2.1}$$

$$\begin{aligned}\frac{\partial u}{\partial t} + v\frac{\partial u}{\partial y} =& \frac{1}{\rho}\frac{\partial p}{\partial x} + \nu\frac{\partial^2 u}{\partial y^2} + g\beta_\tau(T - T_\infty) + g\beta_c(C - C_\infty) \\ &+ \frac{\sigma B_0^2}{\rho}(U - u) - \frac{\nu}{K}(U - u)\end{aligned} \tag{2.2}$$

$$\frac{\partial T}{\partial t} + v\frac{\partial T}{\partial y} = \frac{k}{\rho c_p}\frac{\partial^2 T}{\partial y^2} + \frac{Q}{\rho c_p}(T - T_\infty) \tag{2.3}$$

$$\frac{\partial C}{\partial t} + v\frac{\partial C}{\partial y} = D_m\frac{\partial^2 C}{\partial y^2} - k_r^2(T - T_\infty)^r exp(-\frac{E_a}{RT}) \tag{2.4}$$

The initial and boundary conditions are equally given by:

$$\begin{aligned}&u = U_0, v = v_w(t), T = T_w, C = C_w \ for\ all\ y,\ t \le 0 \\ &u = U_1, T = T_w + A_1 e^{i\omega t}, C = C_w + A_2 e^{i\omega t}, y = 0 \quad \forall \quad t > 0 \\ &u \to U(t), T \to T_\infty, C \to C_\infty\ as\ y \to \infty, y \to \infty,\ t \ge 0\end{aligned} \tag{2.5}$$

where all the physical variables have their meanings as defined in the nomenclature, $A_1,\ A_2 > 0$ and $A_1 = \epsilon(T_w - T_\infty),\ A_2 = \epsilon(C_w - C_\infty)$.

Let us introduce the non-dimensional variables:

$$\begin{aligned}&y' = \frac{yv_0}{v}, u' = \frac{u}{U_0}, t' = \frac{tv_0^2}{4\nu}, U' = \frac{U}{U_0} \\ &\omega' = \frac{4\omega v}{v_0^2}, V = \frac{U_1}{U_0}, \theta = \frac{E_a}{RT_\infty^2}(T - T_\infty)\end{aligned} \tag{2.6}$$

Following Messiha [55], Equation (1) on integration becomes

$$v(t,\ y) = constant$$

But at

$$t = 0, v(t, y) = v_w(t) = -v_0(1 + \epsilon A e^{i\omega t})$$
$$\Rightarrow v(t, y) = -v_0(1 + \epsilon A e^{i\omega t}) \tag{2.7}$$

The stream velocity is given by

$$U(t) = 1 + \epsilon e^{i\omega t}$$

At free stream, $u \to U$,$T \to T_\infty$,$C \to C_\infty$, thus from equation (2)

$$-\frac{1}{\rho}\frac{\partial p}{\partial x} = \frac{\partial U}{\partial t} = \frac{\partial}{\partial t}(1 + \epsilon e^{i\omega t})$$

Using the above and, equations (2.6) and (2.7), equations (2.2)-(2.4) after dropping primes becomes

$$\frac{1}{4}\frac{\partial u}{\partial t} - (1 + \epsilon e^{i\omega t})\frac{\partial u}{\partial y} = \epsilon\frac{i\omega}{4}(e^{i\omega t}) + \frac{\partial^2 u}{\partial y^2} + Gr\tau\theta + Grc\phi - (M + k_p)\cdot(1 - u) \tag{2.8}$$

$$\frac{1}{4}\frac{\partial \theta}{\partial t} - (1 + \epsilon e^{i\omega t})\frac{\partial \theta}{\partial y} = \frac{1}{Pr}\frac{\partial^2 \theta}{\partial y^2} + \delta\theta \tag{2.9}$$

$$\frac{1}{4}\frac{\partial \phi}{\partial t} - (1 + \epsilon e^{i\omega t})\frac{\partial \phi}{\partial y} = \frac{1}{Sc}\frac{\partial^2 \phi}{\partial y^2} - \epsilon\lambda\phi\theta^r e^{\frac{\theta}{1+\epsilon\theta}} \tag{2.10}$$

where λ is the reactivity parameter, δ is heat generation/absorption parameter, M is magnetic parameter, k_p is porosity parameter, other flow governing parameters are as defined in the *nomenclature*.

The non-dimensional parameters governing the flow are define as

$$k_p = \frac{\mu\nu}{(v_0^2 k)}, M = \frac{{\beta_0}^2}{v_0}\frac{\sigma\nu}{\rho}, Sc = \frac{\mu}{Dm}, P_r = \frac{\mu c_p}{k}, \delta = \frac{Q\nu}{v_0^2\rho c_p},$$
$$Grt = \frac{\nu g\beta_\tau}{U_0 v_0^2}(T_w - T_\infty), Grc = \frac{\nu g\beta_\tau}{U_0 v_0^2}(C_w - C_\infty),$$
$$\lambda = \frac{\nu(\epsilon T_\infty)^r}{\epsilon v_0^2}\frac{k_r^2}{e^{\frac{1}{\epsilon}}}, \epsilon = \frac{RT_\infty}{E_a}$$

And the corresponding initial-boundary condition (2.5) becomes

$$y = 0 : u = V, \theta = 1 + e^{i\epsilon\omega t}, \phi = 1 + e^{i\epsilon\omega t}$$
$$y \to \infty : u \to U, \theta \to 0, \phi \to 0 \tag{2.11}$$

3. METHOD OF SOLUTION

To solve equations (2.8) - (2.10) with the initial boundary conditions (2.11), perturbation in the neighborhood of ϵ is used, similar to the one used by Lighthill [56]. The Velocity, specie concentration and temperature fields are given by the expressions

$$\begin{aligned} u(y,t) &= f_0 + \epsilon e^{i\omega t} f_1, \\ \phi(y,t) &= h_0 + \epsilon e^{i\omega t} h_1, \\ \theta(y,t) &= g_0 + \epsilon e^{i\omega t} g_1 \end{aligned} \tag{3.1}$$

3.1 Velocity, Temperature and Concentration Distribution

Substituting equations (3.1) into equation (2.8) - (2.11), separating the harmonic and non-harmonic terms and neglecting the coefficient of ϵ^2, the mean velocity, mean temperature and mean chemical specie respectively are;

$$f_0'' + f_0' + (M + k_p) f_0 = 0, \tag{3.2}$$

$$g_0'' + Pr g_0' + Pr\delta g_0 = 0, \tag{3.3}$$

$$h_0'' + Sc h_0' - Sc\lambda g_0 h_0^r e^{h_0} = 0 \tag{3.4}$$

with boundry conditions

$$\begin{aligned} &y = 0 : f_0 = V,\ g_0 = 1,\ h_0 = 1, \\ &y \to \infty : f_0 \to 0,\ g_0 \to 0,\ h_0 =\to 0 \end{aligned} \tag{3.5}$$

And the oscillatory part of the velocity, temperature and chemical species are

$$f_1'' + f_1' + (M + k_p + \frac{i\omega}{4}) f_1 = \frac{i\omega}{4} - f_0' - Grtg_1 - Grch_1 \tag{3.6}$$

$$g_1'' + Pr g_1' + Pr(\delta - \frac{i\omega}{4}) g_1 = - Pr g_0' \tag{3.7}$$

$$\begin{aligned} h_1'' + Sc h_1' - Sc(\frac{i\omega}{4}\lambda g_0^r e^{g_0}) h_1 = &- Sc h_1' + \lambda Sc h_1 \\ &+ r g_0^{-1} h_0 g_1 g_0^r e^{g_0} \end{aligned} \tag{3.8}$$

Also the corresponding boundary conditions are give by the expressions

$$\begin{aligned} &y = 0 : f_1 = 0,\ g_1 = \ h_1 = 1, \\ &y \to \infty : f_1 \to 0,\ g_1 \to 0,\ h_1 =\to 0 \end{aligned} \tag{3.9}$$

The solutions of equations (3.2)-(3.4) and equations (3.6)- (3.8) under the boundary conditions (3.5) and (3.9) respectively, are

$$g_0(y) = e^{-my} \tag{3.10}$$

$$h_0(y) = e^{-Scy}(1 - \lambda a_0(1 - e^{-my})) \tag{3.11}$$

$$f_0(y) = 1 + a_{13}e^{-cy} + a_{15}e^{-my} + a_{16}e^{-Scy} + a_{17}e^{(m+Sc)y} \tag{3.12}$$

$$g_1(y) = \frac{i\omega}{4}(e^{-m_1 y} - e^{-my}) \tag{3.13}$$

$$\begin{aligned} h_1(y) = {} & ia_1e^{-Scy} + (a_3 + i(a_1 + a_4) + \lambda a_5)e^{-ny} \\ & + (a_3 + ia_4)e^{-(m+Sc)y} + \lambda(a_6e^{-n_2y} + a_7e^{-n_3y} \\ & + a_8e^{-n_4y} + a_9e^{-(n_3+m_1)y} + a_{10}e^{-(n_6+m_1)y} \\ & + a_{11}e^{-(n_2+m_1)y}a_{12}e^{-n_5y}) \end{aligned} \tag{3.14}$$

$$\begin{aligned} f_1(y) = {} & 1 + a_{19}e^{-c_1y} + a_{20}e^{-cy} + a_{21}e^{-my} + a_{22}e^{-Scy} \\ & + a_{23}e^{-m_1y} + a_{24}e^{-(m+Sc)y} + a_{25}e^{-ny} + a_{27}e^{-n_3y} \\ & + a_{28}e^{-n_4y} + a_{29}e^{-(n_4+m_1)y} + a_{30}e^{-(n_6+m_1)y} \\ & + a_{31}e^{-(n_2+m_1)y} + a_{32}e^{-n_5y} \end{aligned} \tag{3.15}$$

where

$$\delta >> \frac{Pr - 1}{Pr} \Rightarrow m << 1,$$

here,

$$\begin{aligned} & n_2 = Sc + m(r + 2), \quad n_3 = m(r + 1) + n1, \quad n_6 = mr + Sc \\ & n_4 = Sc + m(r + 1), \quad n_5 = Sc + m(r + 3), \end{aligned}$$

The functions $f_0(y)$, $g_0(y)$ and $h_0(y)$ presented by equations (3.10) -(3.12) are the mean velocity, the mean temperature and mean concentration fields respectively, and $f_1(y)$, $g_1(y)$ and $h_1(y)$ presented by equations (3.13) -(3.15) are the oscillatory part of the velocity, temperature and concentration respectively.

On substituting equations (3.10) - (3.15) into (3.1), the $2-$ *dimensional* expression for the velocity, concentration and temperature distribution are

$$
\begin{aligned}
u(y,t) &= 1 + a_{13}e^{-cy} + a_{15}e^{-my} + a_{16}e^{-Scy} + a_{17}e^{-(m+Sc)y} \\
&\quad + \epsilon(a_{19}e^{-(c_1+Ic_2)y} + (b_{15}+Ib_{16})e^{-cy} + (b_{17}+Ib_{18})e^{-my} \\
&\quad + (b_{19}+Ib_{20})e^{-Scy} + (b_{21}+Ib_{22})e^{-(d_1+Id_2)y} \\
&\quad + (b_{29}+Ib_{30}e^{-n_3y} + (b_{23}+Ib_{24})e^{-(m+Sc)y} \\
&\quad + (b_{25}+Ib_{26})e^{-ny} + (b_{27}+Ib_{28})e^{-n_2y} \\
&\quad + (b_{31}+Ib_{32})e^{-n_4y} + (b_{33}+Ib_{34})e^{-(n_4+d_1+Id_2)y} \\
&\quad + (b_{35}+Ib_{36})e^{-(n_6+d_1+Id_2)y} + (b_{37}+Ib_{38})e^{-(n_2+d_1+Id_2)y} \\
&\quad + (b_{39}+Ib_{40})e^{-n_5y} + (b_{41}+Ib_{42}))e^{I\omega t}
\end{aligned} \tag{3.16}
$$

$$
\begin{aligned}
\phi(y,t) &= e^{-Scy}(1-\lambda a_0(1-e^{-my})) + \epsilon((a_3+I(a_1+a_4) \\
&\quad + \lambda a_5)e^{-(c_1+Ic_2)y} + (a_3+Ib_4)e^{-(m+Sc)y} + Ia_1e^{-Scy} \\
&\quad + \lambda((b_1+Ib_2)e^{-n_2y} + (b_3+Ib_4)e^{-n_3y} + (b_5+Ib_6)e^{-n_4y} \\
&\quad + (b_7+Ib_8)e^{-(n_4+d_1+Id_2)y} \\
&\quad + (b_9+Ib_{10})e^{-(n_6+d_1+Id_2)y} + (b_{11}+Ib_{12})e^{-(n_2+d_1+Id_2)y} \\
&\quad + (b_{13}+Ib_{14})e^{-n_5y}))e^{I\omega t}
\end{aligned} \tag{3.17}
$$

$$
\theta(y,t) = e^{-my} + \frac{1}{4}I\epsilon\omega(e^{-m_1y} + e^{-my})e^{I\omega t}, \tag{3.18}
$$

Maple package evalc is applied to the above equations to split equations (3.16)-(3.18) into pairs of real and imaginary parts. From equation (3.16), the real part of the velocity can be written in terms of the fluctuating parts as

$$
\begin{aligned}
\Re(u(y,t)) &= 1 + a_{13}e^{-cy} + a_{15}e^{-my} + a_{16}e^{-Scy} \\
&\quad + a_{20}e^{-(m+Sc)y} + \epsilon(u_1\cos\omega t - u_2\sin\omega t), \text{or} \\
\Re(u(y,t)) &= 1 + a_{13}e^{-cy} + a_{15}e^{-my} + a_{16}e^{-Scy} \\
&\quad + a_{17}e^{-(m+Sc)y} + \epsilon|u_{12}|\cos(\omega t + \alpha_3)
\end{aligned} \tag{3.19}
$$

where

$$\begin{aligned} u_1 =& a_{19}e^{-c_1 y}\cos yc_2 + b_{15}e^{-cy} + b_{17}e^{-my} + b_{19}e^{-Scy} \\ &+ b_{21}e^{-d_1 y}\cos d_2 y + b_{22}e^{-d_1 y}\sin d_2 y \\ &+ b_{23}e^{-(m+Sc)y} + b_{25}e^{-ny} + b_{27}e^{-n_2 y} \\ &+ b_{29}e^{-n_3 y} + b_{31}e^{-n_4 y} + b_{33}e^{-(n_4+d_1)y}\cos d_2 y \\ &+ b_{34}e^{-(n_4+d_1)y}\sin d_2 y + b_{35}e^{-(n_6+d_1)y}\cos d_2 y \\ &+ b_{36}e^{-(n_6+d_1)y}\sin d_2 y + b_{37}e^{-(n_2+d_1)y}\cos d_2 y \\ &+ b_{38}e^{-(n_2+d_1)y}\sin d_2 y + b_{39}e^{-n_5 y} + b_{41} \end{aligned} \tag{3.20}$$

$$\begin{aligned} u_2 =& - a_{19}e^{-c_1 y}\sin yc_2 + b_{16}e^{-cy} + b_{18}e^{-my} + b_{20}e^{-Scy} \\ &- b_{21}e^{-d_1 y}\sin d_2 y + b_{22}e^{-d_1 y}\cos d_2 y \\ &+ b_{24}e^{-(m+Sc)y} + b_{26}e^{-ny} + b_{28}e^{-n_2 y} \\ &+ b_{30}e^{-n_3 y} + b_{32}e^{-n_4 y} - b_{33}e^{-(n_4+d_1)y}\sin d_2 y \\ &+ b_{34}e^{-(n_4+d_1)y}\cos d_2 y + b_{35}e^{-(n_6+d_1)y}\sin d_2 y \\ &+ b_{36}e^{-(n_6+d_1)y}\cos d_2 y - b_{37}e^{-(n_2+d_1)y}\sin d_2 y \\ &+ b_{38}e^{-(n_2+d_1)y}\cos d_2 y + b_{40}e^{-n_5 y} + b_{42} \end{aligned} \tag{3.21}$$

$$|u_{12}| = (u_1^2 + u_2^2)^{frac12}, \qquad \tan\alpha_3 = \frac{u_2}{u_1} \tag{3.22}$$

And from (3.17) the expression for concentration field is

$$\begin{aligned} \Re(\phi(y,t)) =& e^{-Scy}(1 - \lambda a_0(1 - e^{-my})) \\ &+ \epsilon(\phi_1\cos\omega t - \phi_2\sin\omega t), \text{or} \\ \Re(\phi(y,t)) =& e^{-Scy}(1 - \lambda a_0(1 - e^{-my})) \\ &+ \epsilon|\phi_{12}|\cos(\omega t + \alpha_2) \end{aligned} \tag{3.23}$$

where

$$\begin{aligned} \phi_1 =& (a_3 + \lambda a_5)e^{-e_1 y}\cos ye_2 + (a_1 + a_4)e^{-e_1 y}\sin e_2 y \\ &+ a_3 e^{-(m+Sc)y} + \lambda(b_1 e^{-n_2 y} + b_3 e^{-n_3 y} + b_5 e^{-n_4 y} \\ &+ (b_7 e^{-n_4 y} + b_9 e^{-n_6 y} + b_{11}e^{-n_2 y})e^{-d_1 y}\cos d_2 y \\ &+ (b_8 e^{-n_4 y} + b_{10}e^{-n_6 y} + b_{12}e^{-n_2 y})e^{-d_1 y}\sin d_2 y \\ &+ b_{13}e^{-n_5 y} \end{aligned} \tag{3.24}$$

$$\begin{aligned}\phi_2 =& a_1 e^{-Scy} + (a_1 + a_4)e^{-e_1 y}\cos e_2 y \\ &- (a_3 + \lambda a_5)e^{-e_1 y}\sin e_2 y + a_4 e^{-(m+Sc)y} + \lambda(b_2 e^{-n_2 y} \\ &+ b_4 e^{-n_3 y} + b_6 e^{-n_4 y} + (b_8 e^{-n_4 y} + b_{10}e^{-n_6 y} \\ &+ b_{12}e^{-n_2 y})e^{-d_1 y}\cos d_2 y + (b_7 e^{-n_4 y} + b_9 e^{-n_6 y} \\ &+ b_{11}e^{-n_2 y})e^{-d_1 y}\sin d_2 y + b_{14}e^{-n_5 y})\end{aligned} \tag{3.25}$$

$$|\phi_{12}| = (\phi_1^2 + \phi_2^2)^{\frac{1}{2}}, \tan\alpha_2 = \frac{\phi_2}{\phi_1} \tag{3.26}$$

Also from equation (3.18), the real part of the temperature field can be written as

$$\begin{aligned}\Re(\theta(y,t)) &= e^{-my}(1 + \frac{1}{4}\epsilon\omega) + \epsilon(\theta_1\cos\omega t - \theta_2\sin\omega t), \text{or} \\ \Re(\theta(y,t)) &= e^{-my}(1 + \frac{1}{4}\epsilon\omega) + \epsilon|\theta_{12}|\cos(\omega t - \alpha_1)\end{aligned} \tag{3.27}$$

where

$$\theta_1 = \frac{1}{4}\omega e^{-d_1 y}\sin\omega t, \qquad \theta_2 = \frac{1}{4}\omega e^{-d_1 y}\cos\omega t, \tag{3.28}$$

$$|\theta_{12}| = (\phi_1^2 + \phi_2^2)^{\frac{1}{2}}, \qquad \tan\alpha_1 = \frac{\theta_2}{\theta_1} \tag{3.29}$$

Note: u_1, u_2, ϕ_1, ϕ_2, θ_1, θ_1 are the fluctuating part of *Skin-Friction*, *Nusselt Number* and *Sherwood Number*.

From (3.19), (3.23) and (3.27) the expression for the transient velocity, transient concentration field and transient temperature were obtained respectively, when $\omega t = \frac{\pi}{2}$, as

$$\begin{aligned}u(y,t) =& 1 + a_{13}e^{-cy} + a_{15}e^{-my} + a_{16}e^{-Scy} \\ &+ a_{17}e^{-(m+Sc)y} - \epsilon u_2\end{aligned} \tag{3.30}$$

$$\phi(y,t)) = e^{-Scy}(1 - \lambda a_0(1 - e^{-my})) - \epsilon\phi_2 \tag{3.31}$$

$$\theta(y,t)) = e^{-my}(1 + \frac{1}{4}\epsilon\omega) - \epsilon\theta_2 \tag{3.32}$$

3.2. Skin - friction, Rate of mass transfer and Heat flux.

Since we know the velocity distribution, we then calculate the skin friction as

$$\tau = \frac{\tau'}{\rho U_0' v_0'} = -\frac{\partial u}{\partial y}\Big|_{y=0}$$

$$\begin{aligned}\tau =&a_{13}c + a_{15}m + a_{17}(m + Sc) + \epsilon(a_{19}(c_1 + Ic_2)\\ &+ (b_{15} + Ib_{16})c + (b_{17} + Ib_{18})m + (b_{19} + Ib_{20})Sc\\ &+ (b_{21} + Ib_{22})(d_1 + Id_2) + (b_{23} + Ib_{24})(m + Sc)\\ &+ (b_{25} + Ib_{26})n + (b_{27} + Ib_{28})n_2 + (b_{29} + Ib_{30})n_4\\ &+ (b_{33} + Ib_{34})(n_4 + d_1 + Id_2) + (b_{35} + Ib_{36})(n_6 + d_1\\ &+ Id_2) + (b_{37} + Ib_{38})(n_2 + d_1 + Id_2)\\ &+ (b_{39} + Ib_{40})n_5)e^{I\omega t}\end{aligned} \tag{3.33}$$

In terms of amplitude and phase of the skin friction, $\Re(\tau)$ is given by

$$\begin{aligned}\Re(\tau) =&a_{13}c + a_{15}m + a_{16}Sc + a_{17}(m + Sc)\\ &- \epsilon(\tau_1 \cos\omega t + \tau_2 \sin\omega t), \text{or}\\ \Re(\tau) =&a_{13}c + a_{15}m + a_{16}Sc + a_{17}(m + Sc) - \epsilon|\tau_{12}| \cos\omega t\end{aligned} \tag{3.34}$$

with

$$\begin{aligned}\tau_1 =&(b_{22} + b_{34} + b_{36} + b_{38})d_2 - a_{19}c_1 - b_{15}c\\ &- b_{17}m - b_{19}Sc + (b_{33} + b_{21} + b_{37})d_1 - b_{23}(m + Sc)\\ &- b_{25}n - b_{27}n_2 - -b_{37}n_3 - (b_{31} + b_{34})n_4 - b_{35}n_5\end{aligned} \tag{3.35}$$

$$\begin{aligned}\tau_2 =&- b_{22}n - b_{28}n_2 - b_{30}n_3 - b_{32})n_4 - b_{40}n_5 - a_{19}c_2\\ &- b_{21}d_2 - b_{22}d_1 - b_{24})(m + Sc) - b_{33}d_2\\ &- b_{36}(n_6 + d_1) - b_{37}d_2 - b_{38}(n_2 + d_1) - b_{16}c\\ &- b_{18}m - b_{20}Sc - b_{34}(n_4 + d_1) - b_{35}d_2\end{aligned} \tag{3.36}$$

$$|\tau_{12}| =(\tau_1^2 + \tau_2^2)^{\frac{1}{2}}, \tan\alpha_6 = \frac{\tau_2}{\tau_1} \tag{3.37}$$

Also since we know the concentration distribution, then the rate of mass transfer at the wall is calculated as

$$Sh =\frac{v\xi_z{}'}{U_0'v_0'}(\frac{\mu_0}{\rho})^{\frac{1}{2}} = \frac{\partial\phi}{\partial y}\ |_{y=0}$$

$$\begin{aligned}Sh =&Sc + \lambda a_0 m - \epsilon(-(a_3 + I(a_1 + a_4) + \lambda a_5)(e_1 + Ie_2)\\ &- (a_3 + Ib_4)(m + Sc) - Ia_1Sc - \lambda((b_1 + Ib_2)n_2\\ &- (b_3 + Ib_4)n_3 - (b_5 + Ib_6)n_4 - (b_7 + Ib_8)(n_4\\ &+ d_1 + Id_2) - (b_9 + Ib_{10})(n_6 + d_1 + Id_2)\\ &- (b_{11} + Ib_{12})(n_2 + d_1 + Id_2) - (b_{13} + Ib_{14})n_5))e^{I\omega t}\end{aligned}$$

And in terms of amplitude and phase of mass transfer at the wall, we have

$$\begin{aligned} \Re(Sh) =& Sc + \lambda a_0 m - \epsilon(sh_1 \cos\omega t + 2\sin\omega t), \qquad \text{or} \\ \Re(Sh) =& Sc + \lambda a_0 m - \epsilon s h_{12} \cos(\omega t - \alpha_5) \end{aligned} \tag{3.38}$$

where

$$\begin{aligned} Sh_1 =& - a_3 e_1 - a_3(m + Sc) - \lambda(b_1 n_2 - b_3 n_3 - b_5 n_4 \\ & - b_7(n_4 + d_1) - b_9(n_6 + d_1) - b_{11}(n_2 + d_1) - b_{13} \\ & n_5 + (b_8 + b_{10} + b_{12})d_2 + (a_1 + a_4)e_2 - a_5 e_1) \end{aligned} \tag{3.39}$$

$$\begin{aligned} Sh_2 =& - a_3 e_2 - a_1(e_1 + Sc) - a_4 e_1 - a_4(m + Sc) \\ & - \lambda(b_2 n_2 - b_4 n_3 - b_6 n_4 - b_8(n_4 + d_1) - b_{10}(n_6 + d_1) \\ & - b_{12}(n_2 + d_1) - b_{14} n_5 + (b_7 + b_{11} + b_9)d_2 \\ & + (a_1 + a_4)e_2 - a_5 e_2) \end{aligned} \tag{3.40}$$

$$|Sh_{12}| = (Sh_1^2 + Sh_2^2)^{\frac{1}{2}},\ \tan\alpha_5 = \frac{Sh_2}{Sh_1} \tag{3.41}$$

Finally, expression for heat transfer at the wall is written as

$$\begin{aligned} Nu =& -\frac{\partial\theta}{\partial y}|_{y=0}, \\ Nu =& m + \frac{1}{4} I\epsilon\omega(d_1 + Id_2 + m)e^{I\omega t}, \end{aligned}$$

In terms of amplitude and phase of the skin friction, we have

$$\begin{aligned} \Re(Nu) &= m - \epsilon(Nu_1 \cos\omega t - Nu_2 \sin\omega t), \text{ or} \\ \Re(Nu) &= m - \epsilon Nu_{12} \cos(\omega t - \alpha_4) \end{aligned} \tag{3.42}$$

where

$$Nu_1 = \frac{1}{4}\epsilon\omega d_2, Nu_2 = \frac{1}{4}\epsilon\omega m - d_1) \tag{3.43}$$

$$|Nu_{12}| = (Nu_1^2 + Nu_2^2)^{\frac{1}{2}} = \frac{1}{4}\epsilon\omega(d_2^2 + (m - d_1)^2)^{\frac{1}{2}} \tag{3.44}$$

$$\tan\alpha_4 = \frac{Nu_2}{Nu_1} = \frac{d_2}{m - d_1} \tag{3.45}$$

Where tau_1, tau_2, Sh_1, Sh_2, Nu_1, Nu_1 are the fluctuating part of *Skin-Friction*, *Nusselt Number* and *Sherwood Number*.
Here also, the expression for the transient Skin-Friction, transient Sherwood Number and transient Nusselt Number were obtained

respectively, when $\omega t = \frac{\pi}{2}$ from (3.33), (3.37) and (3.41), as

$$\tau = a_{13}c + a_{15}m + a_{16}Sc + a_{17}(m + Sc) - \epsilon\tau_2, \tag{3.46}$$

$$Sh = Sc + \lambda a_0 m - \epsilon sh_2, \tag{3.47}$$

$$Nu = m + \epsilon Nu_2 \tag{3.48}$$

4. DISCUSSION

For the purpose of discussing the effect of various governing parameters on the flow behavior, calculations have been carried out for different values of V, M, k_p, Grt, Grc, r and, for fixed values of Sc, Pr and ϵ. In order to point out the effects of these parameters on flow characteristic, to be realistic, the value of Prandtl number is chosen to be $Pr = 0.71$ and $Sc = 0.62$ which represents air at temperature 25^oC and one atmospheric pressure. All parameters are primarily chosen as follows: $V = 0.3$, $M = 0.2$, $k_p = 0.5$, $\delta = 0.2$, $Grt = 0.5$, $Grc = 0.2$, $\lambda = 0.1$, $r = 1.0$ and $\omega = \pi t$ unless otherwise stated. Equations ((3.20)-(3.22)), ((3.22)-(3.26)) and ((3.28)-(3.29)) gives the expressions for fluctuating part, amplitude and phase of velocity, concentration and temperature profile respectively, transient velocity, concentration and temperature are given by equations ((3.30) - (3.33)) while the transient skin-friction, mass and heat transfer at wall are respectively given by equations (3.45)-(3.47).

4.1 Temperature, Concentration and Velocity distributions
In Fig. 4.1.1, the transient temperature field is displayed with various values of angular velocity ω. It is observed that temperature increases as the fluid angular velocity increases and temperature boundary layer decreases as the fluid moves away from the plate which asymptotically approaches zero far away from the plate. The presence of peak in the profile indicates that maximum temperatures exist in the body of fluid. Also, temperature boundary layer increases with an increase in ω. It was seen that maximum velocity occur when $\omega > 45$. This maximum is given by $\frac{\omega^2+16}{16(4\epsilon+1)}$. Fig. 4.1.2 shows that the thermal boundary layer increases for an increase in Pr, $0 < Pr < 1$ but decreases as Prandtl number increases for $Pr \geq 4$. It should also be mentioned that temperature increases for an increase in heat generation (i.e $\delta > 0$) and vice-versa. Fig. 4.1.3 depict the effect of Prandtl number on fluctuating part of the temperature. comparing the curves in the profile, it could be seen that the highest fluctuation in temperature occurs with lowest

value of Prandtl number which implies higher thermal conductivity. That is fluctuation reduces as viscosity increases, the lower the thermal conductivity compare to viscosity, the lower the fluctuation. Figs. 4.1.4 and 4.1.5 depicts the effects of angular frequency and Prandtl number respectively, on amplitude of temperature distribution. From these figures it is observed that increase in angular frequency brings about increase in amplitude of temperature while increase in Prandtl number diminish the amplitude of temperature. While in Fig. 4.1.6, the effect of Prandtl number on phase of temperature distribution is displayed, from where it is observed that increase in thermal conductivity increases the phase of temperature while increase in viscosity diminish phase of temperature. Transient concentration distribution variation with respect to chemical reactivity parameter is shown in Fig. 4.1.7, it could be seen that concentration increases with an increase in generative chemical reaction and decrease with increase in destructive chemical reaction. It is also observe that for higher value of negative λ, corresponding to generative chemical reaction, maximum concentration exist in the body of the fluid close to the surface. In Fig. 4.1.8, show that chemical specie boundary layer decreases with an increase in reaction order. The effect of reaction order on the flow becomes negligible when $r \geq 3$. Figs. 4.1.9 and 4.1.10 depicts the effect of reactivity parameter and reaction. From both figures, indicate that increase in chemical reaction parameter increases the amplitude of concentration for both generative and destructive chemical reaction while increase in reaction order diminish the amplitude of concentration. Figs. 4.1.11 and 4.1.12 depict the effect of chemical reaction parameter and reaction order. From Fig. 4.1.11, increase in chemical reaction increases the phase of concentration, this phenomenon reverses at a regular pattern. The transient velocity profiles are shown in Figs 4.1.13 - 4.1.19 for different values of reactivity parameter λ, limiting surface velocity V, thermal and mass Grashof numbers Grc, Grt, reaction order r permeability parameter k_p and magnetic parameter M respectively. From Fig. 4.1.13, it could be seen that transient velocity decrease with increase in generative chemical reaction and increases with an increase in destructive chemical reaction. From Fig. 4.1.14, the transient velocity increases when the limiting surface moves in the positive direction of the flow, whereas it decreases when it moves in the opposite direction. The effect of mass Grashof number was shown in Fig. 4.1.5, from this

figure, the velocity decreases with increase in mass Grashof number, while Fig. 4.1.16 depict variation of velocity distribution for various values of thermal Grashof number. Comparing the curves in the figure, velocity decreases for an increase in thermal Grashof number for heating of the plate ($Grt > 0$), while for cooling of the plate ($Grt < 0$) resulted in velocity increase as cooling of the plate increases. Also from Figs. 4.1.17 and 4.1.18, increase in reaction order decreases the transient velocity and increases with increase in permeability parameter. It is also deduced from Fig. 4.1.19 that velocity boundary layer increase with an increase in magnetic parameter until a steady state is reached where further increase in not significant. Fig. 4.1.20 depict that for cooling of the plate, the velocity fluctuating part increases while it diminish with an increase for the heating of the plate. The effect of chemical reactivity parameter on velocity fluctuating part displayed in Fig. 4.1.21. show that for generative chemical reaction the velocity fluctuation increases. Fig. 4.1.22 depict that velocity fluctuating part increase when impulse velocity of the limiting surface is in the same direction as the that of the flow while it diminish when impulse velocity of the limiting surface is in a direction opposite that of the flow. Figs. 4.1.23 - 4.1.25 depict the effect of reactivity parameter, impulse velocity of limiting surface and magnetics parameters on phase of velocity respectively. From these figures, it could be seen that both generative chemical reaction and impulse velocity of the limiting surface moves is in the same direction as the that of the flow increase the phase of the velocity while both destructive chemical reaction and impulse velocity of the limiting surface moves is in a direction opposite that of the flow diminish the phase of the velocity and increase in magnetic parameter increase the phase of the velocity.

4.2. Nusselt Number, Sherwood Number and Skin Friction.

Fig. 4.2.1 depict the effect of Prandtl number on rate of heat transfer at the wall. From the figure, increase in viscosity (higher viscosity compare to thermal conductivity) diminish the rate of heat transfer at the wall. The phase of heat transfer at wall is seen to increase with an increase in Prandtl number. This is so because the higher the viscosity the higher the phase of heat transfer at the wall as shown in Fig. 4.2.2.

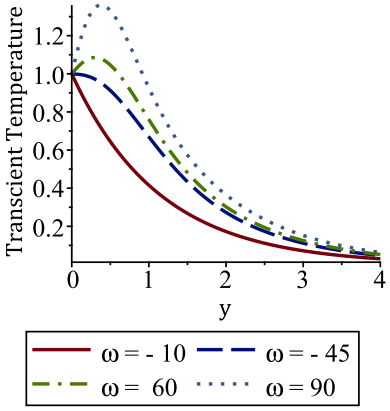

Fig. 4.1.1. Transient temperature distribution at different values of ω.

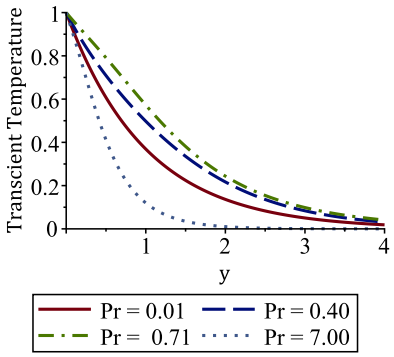

Fig. 4.1.2. Transient temperature distribution at different vlues of Pr.

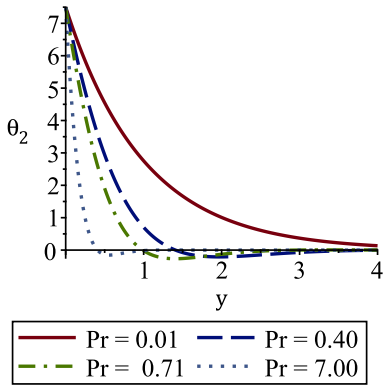

Fig. 4.1.3. Temperature fluctuating part for various values of Pr.

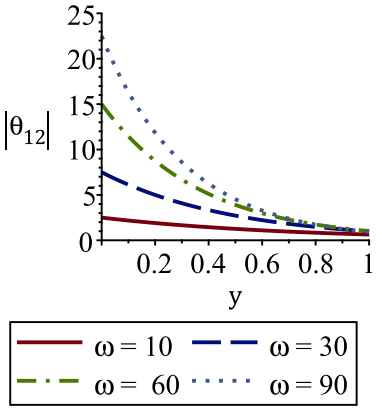

Fig. 4.1.4. Amplitude of Temperature at different values of ω.

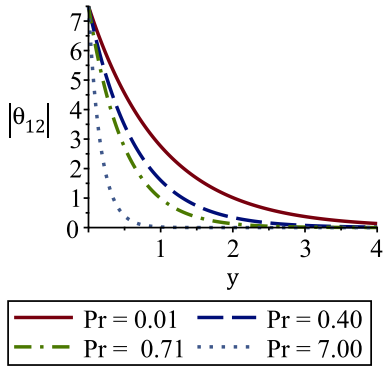

Fig. 4.1.5. Amplitude of Temperature at different values of Pr.

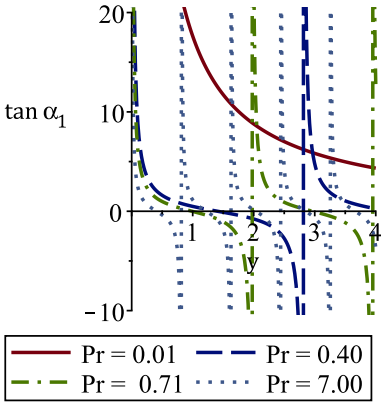

Fig. 4.1.6. Phase of Temperature at different values of Pr.

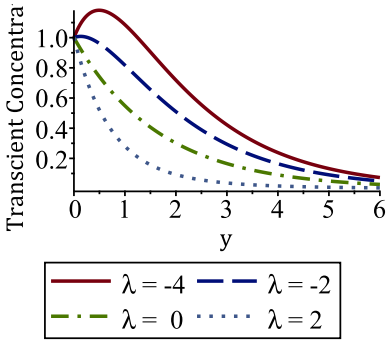

Fig. 4.1.7. Transient Concentration profile for different values of λ.

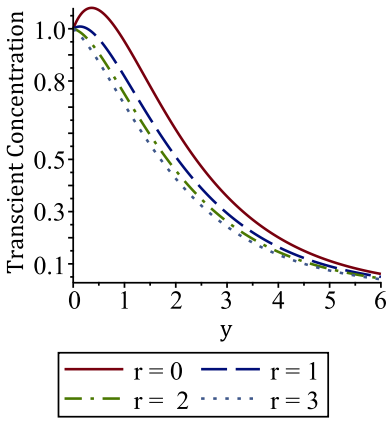

Fig. 4.1.8. Transient Concentration profile for different values of r.

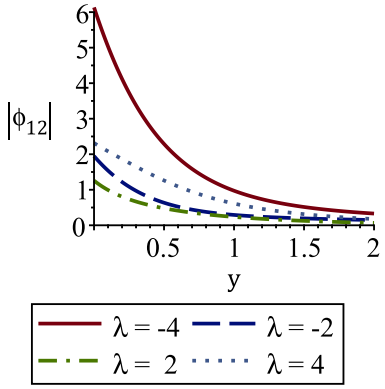

Fig. 4.1.9. Amplitude of Concentration at different values of λ.

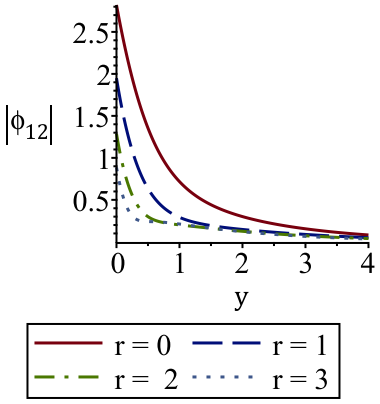

Fig. 4.1.10. Amplitude of Concentration at different values of r.

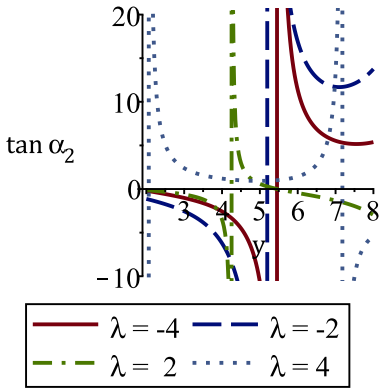

Fig. 4.1.11. Phase of Concentration at different values of λ.

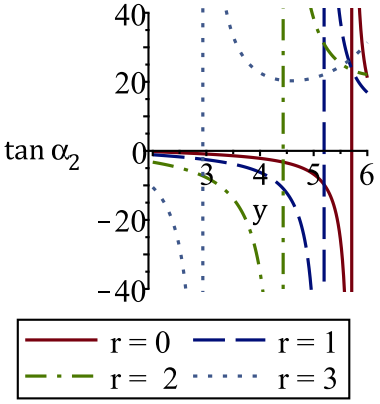

Fig. 4.1.12. Phase of Concentration at different values of λ.

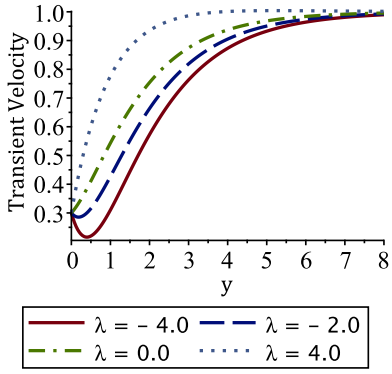

Fig. 4.1.13. Transient velocity profile at different values of λ.

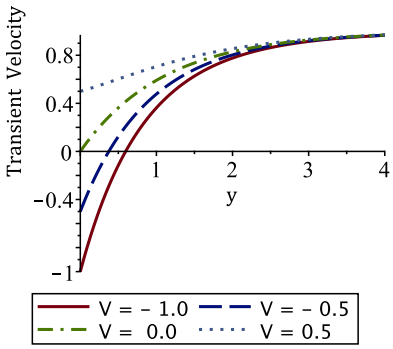

Fig. 4.1.14. Transient velocity profile at different values of V.

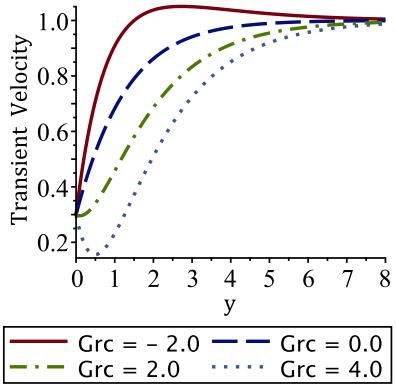

Fig. 4.1.15. Transient velocity profile at different values of Grc.

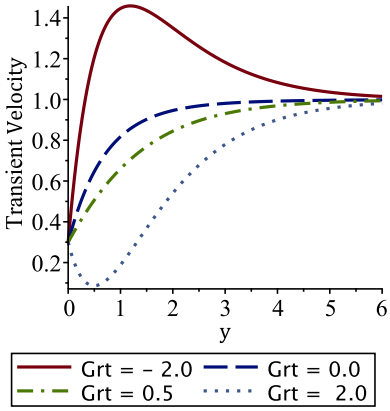

Fig. 4.1.16. Transient velocity profile at different values of Grt.

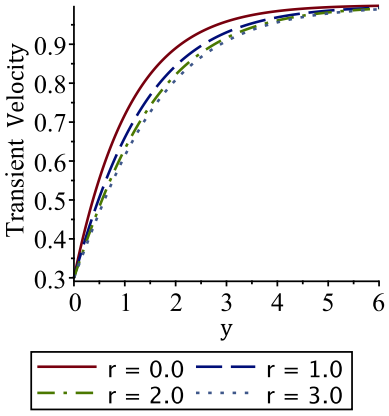

Fig. 4.1.17. Transient velocity profile at different values of r.

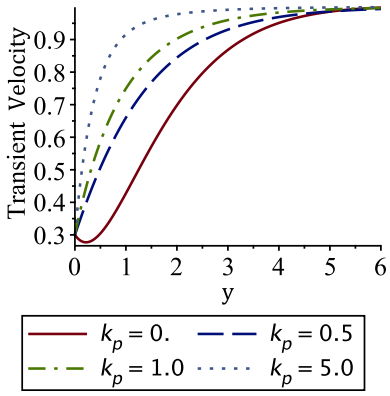

Fig. 4.1.18. Transient velocity profile at different values of k_p.

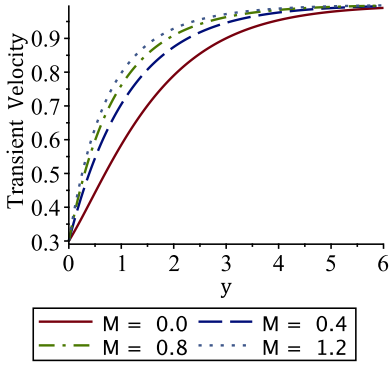

Fig. 4.1.19. Transient velocity profile at different values of M.

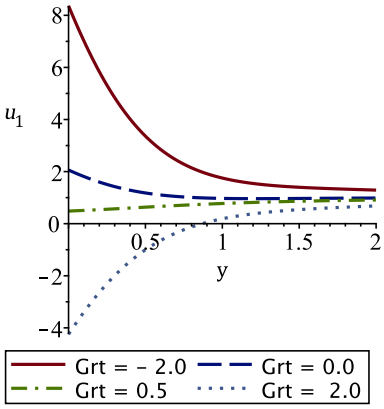

Fig. 4.1.20. Fluctuating part of Velocity distribution at different values of Grt.

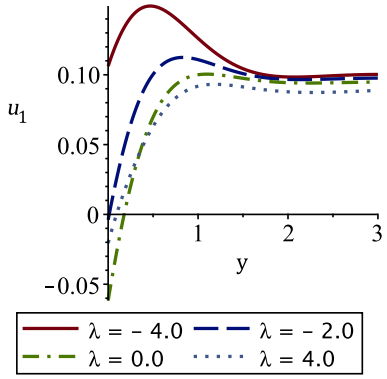

Fig. 4.1.21. Fluctuating part of Velocity distribution at different values of λ.

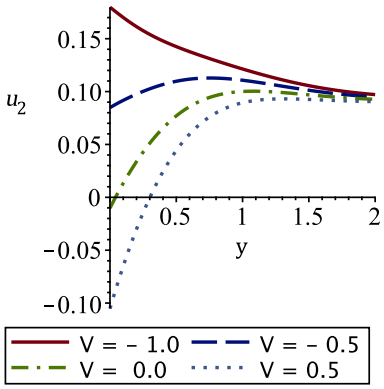

Fig. 4.1.22. Fluctuating part of Velocity distribution at different values of V.

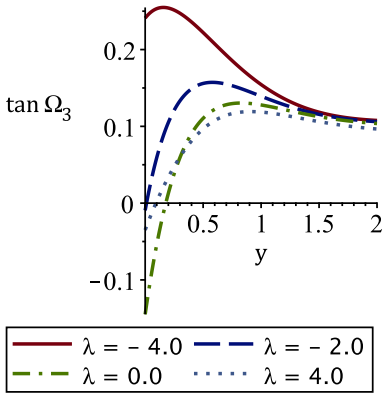

Fig. 4.1.23. Phase of velocity profile for different values of λ.

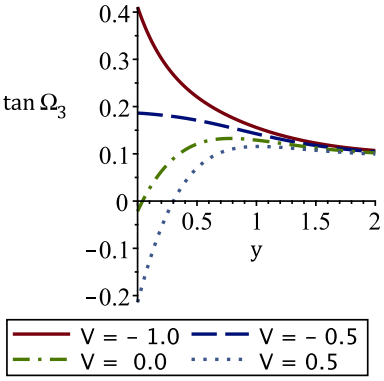

Fig. 4.1.24. Phase of velocity profile for different values of V.

This is so because the higher the viscosity the higher the phase of heat transfer at the wall as shown in Fig. 4.2.2. Mass transfer rate, amplitude and phase of mass transfer rate at the wall is depicted Figs. 4.2.3, 4.2.4 and 4.2.5 respectively. Comparing the curves under the figures, it could be seen that rate of mass transfer rate diminish with an increase in generative chemical reaction while it increase with destructive chemical reaction. Amplitude of mass transfer rate also diminish with increase in reaction order as shown by figure 4.2.4. While it is observed from from Fig. 4.2.5 that phase of mass transfer rate increase with an increase in generative chemical reaction and diminish with increase in destructive chemical reaction. The Skin Friction increase with either increase in destructive chemical reaction or cooling of the plate and diminish with diminish with either increase in generative chemical reaction or heating of the plate as shown in Figs 4.2.6 and 4.2.7 respectively. The fluctuating part of skin-friction for various values of reactivity parameter and surface limiting velocity is displayed in Figs. 4.2.8 and 4.2.9 respectively. From the figures, the fluctuating part of skin-friction is seen to increase with an increase in either generative chemical reaction or impulse velocity of the limiting surface moves in the same direction as that of the flow, and diminish when either destructive chemical reaction increase or impulse velocity of the limiting surface is in a direction opposite to that of the flow. Figs. 4.2.10 depict that increase in mass buoyancy brings increase in amplitude of skin-friction while Fig 4.2.11 shows that phase of skin friction diminish as generative chemical reaction parameter increase.

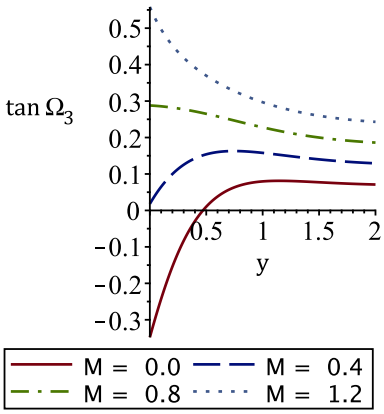

Fig. 4.1.25. Phase of velocity profile for different values of M.

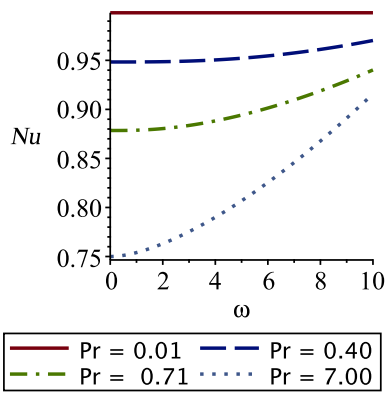

Fig. 4.2.1. Skin-Friction profile for different values of Pr.

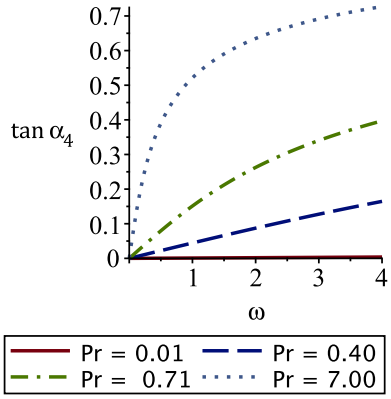

Fig. 4.2.2. Phase of Heat Transfer Rate at the wall profile for different values of Pr.

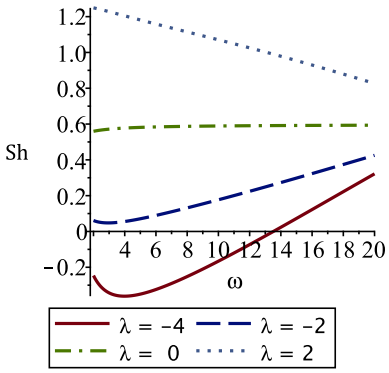

Fig. 4.2.3. Mass transfer rate at wall for different values of λ.

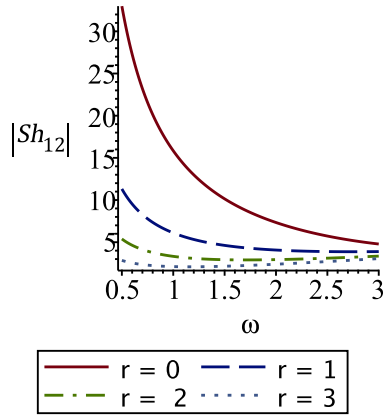

Fig. 4.2.4. Fluctuating part of mass transfer at wall for different values of r.

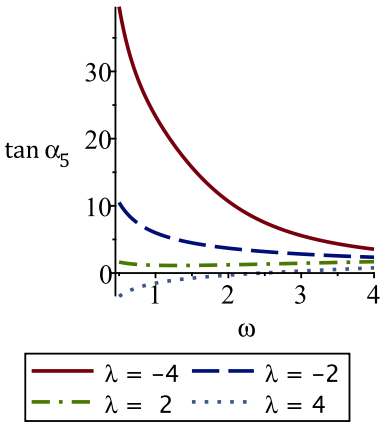

Fig. 4.2.5. Phase of mass transfer at wall for different values of M.

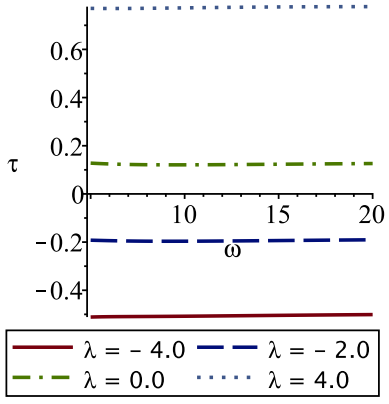

Fig. 4.2.6 Skin-friction profile for different values of λ.

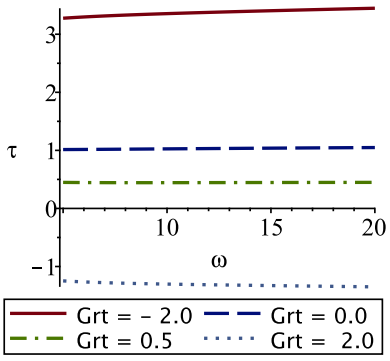

Fig. 4.2.7. Skin-friction profile for different values of Grt.

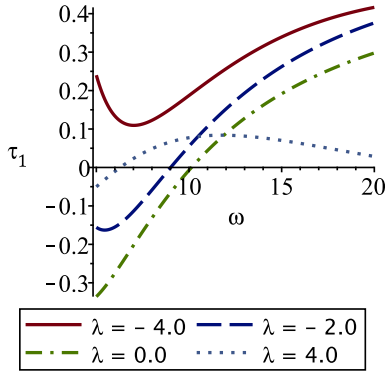

Fig. 4.2.8. Fluctuating part of Skin-Friction for different values of λ.

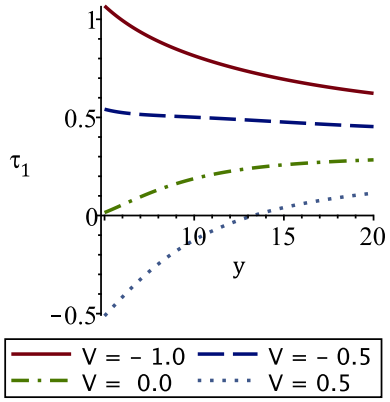

Fig. 4.2.9. Fluctuating part of Skin-Friction for different values of V.

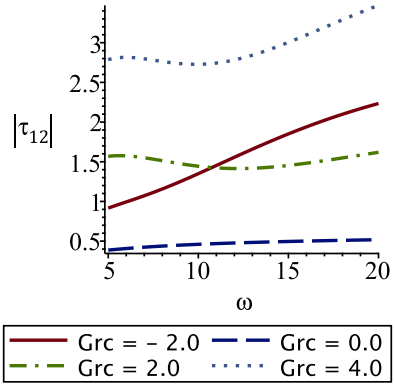

Fig. 4.2.10. Amplitude of Skin-Friction for different values of Grc.

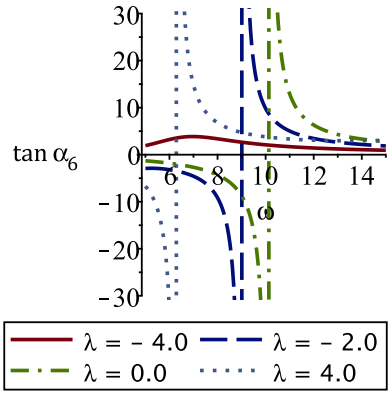

Fig. 4.2.11. Phase of Skin-Friction for different values of λ.

5. CONCLUSION

This paper have studied analytically heat and mass transfer in unsteady natural convection MHD boundary layer flow past a moving plate with mass transfer and a binary chemical reaction. The fluid limiting surface is moved impulsively, with a constant velocity, either in the direction of the flow or in the opposite direction, in the presence of a transverse magnetic field. With oscillating fluid flow, both frequency-dependent effects and "long-time" effects that would require non-practically long channels to be observed in steady flow were studied. Mathematical important aspects of reaction engineering in reactive flow, especially residence time flow behaviour, scale-up and scale-down procedures is also considered. From the present study the following conclusions can be drawn:

- temperature increases as the fluid angular velocity increases
- maximum temperatures exist in the body of the fluid.
- thermal boundary layer decreases as Prandtl number increases.
- concentration increases with an increase in generative chemical reaction and vice-versa.
- transient velocity decrease with increase in generative chemical reaction and reaction order and increases when the limiting surface moves in the positive direction of the flow
- velocity decreases with increase in mass buoyance and thermal Grashof number for heating of the plate
- Skin-friction increases as generative/destructive chemical reaction increases
- Skin friction increases as limiting surface moves in opposite direction and decrease limiting surface moves in the same direction as the fluid flow
- increase in thermal, mass buoyancy and reaction order decreases the skin friction
- skin-friction increase with an increase in Pr or ω and decrease with an increase in A

ACKNOWLEDGMENTS

The authors would like to thank the anonymous referee whose comments improved the original version of this manuscript.

NOMENCLATURE

u	nondimensional fluid axial velocity	Ea	activation energy
T	nondimensional fluid temperature	r	reaction order
C	non - dimensional concentration	K	porosity coefficient
y	transverse coordinate	k	thermal conductivity
ω	frequeesncy of free–stream oscillation	x	horizontal axis
v	fluid transverse velocity	ν	fluid viscosity
Q	heat generation/absorption coefficient	ρ	density
R	universal gas constant	Grt	thermal Grashof number
g	acceleration due to gravity	Grc	mass Grashof number
σ	the electrical conductivity	Pr	Prandtl number
c_p	specific heat at constant pressure	Sc	Schmidt number
D_m	is mass diffusivity	p	pressure
T_w	temperature at the wall	U_∞	wall velocity
B_0	applied magnetic field	i	complex identity
k_r	reactivity of chemical reaction	t	time
C_w	concentration at the wall	$_w$	condition at wall
β_τ	thermal buoyancy term	$_\infty$	ambient condition
β_c	mass buoyancy term		

APPENDIX

$$m = \frac{Pr + \sqrt{Pr^2 - 4Pr\delta}}{2}, \qquad m_1 = \frac{Pr + \sqrt{Pr^2 - 4Pr(\delta - i\frac{\omega}{4})}}{2}$$

$$n = \frac{Sc + \sqrt{(Sc^2 + 4\alpha Sc)}}{2}, \qquad n_1 = \frac{Sc + \sqrt{Sc^2 + 4Sc(\alpha + i\omega Sc)}}{2}$$

$$c = \frac{1 + \sqrt{1 + 4(M + k_p)}}{2}, \qquad c1 = \frac{1 + \sqrt{1 + 4(M + k_p + i\frac{\omega}{4}}}{2}$$

$$a_0 = \frac{e^1 Sc}{m(m + Sc)(r + 2)}, \qquad a_1 = \frac{4ASc}{\omega}(1 - \lambda a_0),$$

$$a_3 = \frac{Am\lambda Sca_0(m + Sc)^2}{m^2(m + Sc)^2 + (\frac{\omega Sc}{4})^2}, \qquad a_5 = -(a_6 + a_7 + \cdots + a_1 2)$$

$$a_4 = \frac{Am\lambda Sc^2 a_0(m + Sc)}{4(m^2(m + Sc)^2 + (\frac{\omega Sc}{4})^2)}, \qquad a_6 = \frac{e^1 Sc(a_3 + ia_4 + (1 - \lambda a_0)\frac{i\omega}{4}}{n_2^2 - n_2 Sc - \frac{i\omega Sc}{4}}$$

$$a_7 = \frac{e^1 Sc(a_3 + i(a_1 + a_4))}{n_3^2 - n_3 Sc - \frac{i\omega Sc}{4}}, \qquad a_9 = \frac{ie^1 Sc(1 + \lambda a_0(r - 1)\frac{\omega}{4}}{(n_4 + m_1)^2 - (n_4 + m_1)Sc - \frac{\omega Sc}{4}}$$

$$a_8 = \frac{e^1 Sc(a_1 - \frac{\omega}{4})}{n_4^2 - n_4 Sc - \frac{i\omega Sc}{4}}, \qquad a_{10} = \frac{ire^1 Sc(1 - \lambda a_0 \frac{\omega}{4})}{(n_6 + m_1)^2 - (n_6 + m_1)Sc - \frac{i\omega\ Sc}{4}}$$

$$a_{11} = \frac{ire^1 Sc\lambda a_0 \frac{\omega}{4}}{(n_2 + m_1)^2 - (n_2 + m_1)Sc - i\frac{\omega Sc}{4}}, \qquad a_{12} = \frac{e^1 Sc\lambda a_0 \omega}{4n_2^2 - 4n_2 Sc - i\omega Sc},$$

$$a_{13} = V - (1 + a_1 5 + a_1 6 + a_1 7), \qquad a_{15} = -\frac{Grt}{m^2 - m + M + k_p},$$

$$a_{17} = -\frac{Grc\lambda a_0}{(m + Sc)^2 - (m + Sc) + M + k_p}, \qquad a_{16} = -\frac{Grc(1 - \lambda a_0)}{Sc^2 - Sc + M + k_p}$$

,

$$a_{19} = -(1 + a_{20} + a_{21} + \cdots + a_{32})$$

$$a_{21} = -\frac{cAa_{15} - i\omega Grt}{4((m^2 - m) - c + M + k_p) + i\omega}, \qquad a_{20} = -\frac{cAa_{13}}{c^2 - c + M + k_p + \frac{i\omega}{4}}$$

$$a_{22} = -\frac{ScAa_{16} - ia_1 Grc}{Sc^2 - Sc + M + k_p + \frac{i\omega}{4}}, \qquad a_{23} = -\frac{i\omega Grt}{4((m_1^2 - m) + M + k_p) + i\omega}$$

$$a_{24} = -\frac{A(m + Sc) - Grc(a_3 - ia_4)}{(m + Sc)^2 - (m + Sc) + M + k_p + \frac{i\omega}{4}}, \qquad a_{25} = -\frac{-Grc(a_3 + i(a_1 + a_4) + \lambda a_5)}{n^2 - n + M + k_p + \frac{i\omega}{4}}$$

$$a_{26} = -\frac{\lambda a_6 Grc}{n_2^2 - n_2 + M + k_p + \frac{i\omega}{4}}, \qquad a_{27} = -\frac{\lambda a_4 Grc}{n_3^2 - n_3 + M + k_p + \frac{i\omega}{4}}$$

$$a_{29} = -\frac{\lambda a_9 Grc}{(n_4 + m_1)^2 - (n_4 + m_1) + M + k_p + \frac{i\omega}{4}}, \qquad a_{28} = -\frac{\lambda a_8 Grc}{n_4^2 - n_4 + M + k_p + \frac{i\omega}{4}}$$

$$a_{30} = -\frac{\lambda a_{10} Grc}{(n_6 + m_1)^2 - (n_6 + m_1) + M + k_p + \frac{i\omega}{4}}, \qquad a_{32} = -\frac{\lambda a_{12} Grc}{n_5^2 - n_5 + M + k_p + \frac{i\omega}{4}},$$

$$a_{31} = -\frac{\lambda a_{11} Grc}{(n_2 + m_1)^2 - (n_2 + m_1) + M + k_p + \frac{i\omega}{4}}, \qquad a_{33} = -\frac{i\omega}{4(M + k_p) + i\omega}$$

We define

$$a_i = b_j + Ib_k, \forall i = 6, 7, \cdots, 32, j = 1, 3, \cdots, 41, k = 2, 4, \cdots, 42$$

$$b_1 = \frac{a_3(n_2^2 - n_2Sc)^2 - \frac{1}{4}(\frac{1}{4}e(1-\lambda a_0)\omega Sc + a_4)\omega Sc}{(n_2^2 - n_2Sc)^2 + \frac{1}{16}\omega^2\omega Sc\omega^2}$$

$$b_2 = \frac{(n_2^2 - n_2Sc)(\frac{1}{4}e(1-\lambda a_0)\omega Sc + a_4)\omega Sc - \frac{1}{4}a_3\omega Sc}{(n_2^2 - n_2Sc)^2 + \frac{1}{16}\omega^2\omega Sc\omega^2}$$

$$b_3 = \frac{(n_3^2 - n_3Sc)(a_3 + a_4)eSc - \frac{1}{4}ea_1\omega\omega Sc\omega^2}{(n_2^2 - n_2Sc)^2 + \frac{1}{16}\omega^2\omega Sc\omega^2}$$

$$b_4 = \frac{(n_3^2 - n_3Sc)eSca_1 + \frac{1}{4}e(a_3 + a_4)\omega\omega Sc\omega^2}{(n_2^2 - n_2Sc)^2 + \frac{1}{16}\omega^2\omega Sc\omega^2}$$

$$b_5 = -\frac{1}{4}\frac{e(a_1 - \frac{1}{4}\omega)\omega\omega Sc\omega^2}{(n_2^2 - n_2Sc)^2 + \frac{1}{16}\omega^2\omega Sc\omega^2} \quad b_6 = \frac{IeSc(a_1 - \frac{1}{4}\omega)(n_2^2 - n_2Sc)^2}{(n_2^2 - n_2Sc)^2 + \frac{1}{16}\omega^2\omega Sc\omega^2}$$

$$b_7 = \frac{\frac{1}{4}(eSc(\lambda a_0(r-1)+1)\omega(2d_2(n_4 + d_1 - Sc) - \frac{1}{4}\omega Sc))}{\omega(d_1^2 + 2d_1n_4 - d_2^2 - Sc(d_1 + n_4) + n_4^2)\omega^2 + (2d_2(n_4 + d_1 - Sc) - \frac{1}{4}\omega Sc)^2}$$

$$b_8 = \frac{\frac{1}{4}(IeSc(\lambda a_0(r-1)+1)\omega(d_1^2 + 2d_1n_4 - d_2^2 - Sc(d_1 + n_4) + n_4^2))}{(d_1^2 + 2d_1n_4 - d_2^2 - Sc(d_1 + n_4) + n_4^2)^2 + (2d_2(n_4 + d_1 - Sc) - \frac{1}{4}\omega Sc)^2}$$

$$b_9 = \frac{\frac{1}{4}(erSc(\lambda a_0 + 1)\omega(2d_2(n_6 + d_1 - Sc) - \frac{1}{4}\omega Sc))}{(d_1^2 + 2d_1n_6 - d_2^2 - Sc(d_1 + n_6) + n_6^2)^2 + (2d_2(n_6 + d_1 - Sc) - \frac{1}{4}\omega Sc)^2}$$

$$b_{10} = \frac{\frac{1}{4}(erSc(1-\lambda a_0)\omega((2d_1n_6 + d_1^2 - d_2^2 + n_6^2 - Sc(d_1 + n_6)) - \frac{1}{4}\omega Sc))}{(d_1^2 + 2d_1n_6 - d_2^2 - Sc(d_1 + n_6) + n_6^2)^2 + (2d_2(n_6 + d_1 - Sc) - \frac{1}{4}\omega Sc)^2}$$

$$b_{11} = \frac{\frac{1}{4}(eSc\lambda a_0\omega(2d_1d_2 - Scd_2 + 2n_2d_2 - \frac{1}{4}\omega Sc))}{(d_1^2 + 2d_1n_2 - d_2^2 - Sc(d_1 + n_2) + n_2^2)^2 + (d_2(2n_2 + \omega 2d\omega_1 - Sc) - \frac{1}{4}\omega Sc)^2}$$

$$b_{12} = \frac{\frac{1}{4}(eSc\lambda a_0\omega(2d_1n_2 - Sc(d_1 + n_2) + d_1^2 - d_2^2 + n_1^2))}{(d_1^2 + 2d_1n_2 - d_2^2 - Sc(d_1 + n_2) + n_2^2)^2 + (d_2(2n_2 + \omega 2d\omega_1 - Sc) - \frac{1}{4}\omega Sc)^2}$$

$$b_{13} = \frac{1}{16}\frac{(e\omega Sc\omega^2\lambda a_0\omega^2}{(n_2^2 - n_2Sc)^2 + \frac{1}{16}\omega^2\omega Sc\omega^2} \qquad b_{14} = \frac{1}{4}\frac{eSc\lambda a_0\omega(n_2Sc + n_2^2)}{(n_2^2 - n_2Sc)^2 + \frac{1}{16}\omega^2\omega Sc\omega^2}$$

$$a_5 = a_6 + a_7 + a_8 + a_9 + a_{10} + a_11 + a_{12} \qquad b_{15} = \frac{Aa_13c(c^2 + M - c + k_p)}{(c^2 + M - c + k_p)^2 + \frac{1}{16}\omega^2}$$

$$b_{16} = \frac{\frac{1}{4}cAa_13\omega}{(c^2 + M - c + k_p)^2 + \frac{1}{16}\omega^2} \qquad b_{17} = \frac{Ama_15(4m^2 + M - 4m + k_p) - \omega^2 Grt}{(4m^2 + M - 4m + k_p)^2 + \omega^2}$$

$$b_{18} = -\frac{\omega Grt(4m^2 + M - 4m + k_p) + Ama_15\omega}{(4m^2 + M - 4m + k_p)^2 + \omega^2}$$

$$b_{19} = \frac{Ama_16(\omega Sc\omega^2 + M - Sc + k_p) - \frac{1}{4}a_1\omega Grc}{(\omega Sc\omega^2 + M - Sc + k_p)^2 + \omega^2}$$

$$b_{20} = \frac{-a_1Grc(\omega Sc\omega^2 + M - Sc + k_p) - \frac{1}{4}a_16mA\omega}{(\omega Sc\omega^2 + M - Sc + k_p)^2 + \omega^2}$$

$$b_{21} = \frac{-\omega Grc(8d_1d_2 + \omega + 4d_2) - \frac{1}{4}a_16mA\omega}{16(d_1^2 - d_2^2 + 4M - d_1 + k_p)^2 + (8d_1d_2 + \omega - 4d_2)^2}$$

$$b_{22} = -\frac{I\omega Grt(d_1^2 - d_2^2 + 4M - d_1 + k_p)}{16(d_1^2 - d_2^2 + 4M - d_1 + k_p)^2 + (8d_1d_2 + \omega - 4d_2)^2}$$

$$b_{23} = \frac{(ASc + Am - a_3Grc)((m + Sc)^2 - (m + Sc) + k_p) - a_4\omega Grc}{((m + Sc)^2 - (m + Sc) + k_p)^2 + \frac{1}{16}\omega^2}$$

$$b_{24} = \frac{-a_4Grc((m + Sc)^2 - (m + Sc) + k_p) - \frac{1}{4}(ASc + Am - a_3Grc)\omega Grc}{((m + Sc)^2 - (m + Sc) + k_p)^2 + \frac{1}{16}\omega^2}$$

$$b_{25} = \frac{-Grc(a_3+\lambda a_5)(n^2-n+M+k_p) - \frac{1}{4}(a_1+a_4)\omega Grc}{(n^2-n+M+k_p)^2+\frac{1}{16}\omega^2}$$

$$b_{26} = \frac{-Grc(a_1+a_4)(n^2-n+M+k_p) - \frac{1}{4}(a_3+\lambda a_5)\omega Grc}{(n^2-n+M+k_p)^2+\frac{1}{16}\omega^2}$$

$$b_{27} = \frac{-a_5 Grc\lambda(n^2-n+M+k_p)}{(n^2-n+M+k_p)^2+\frac{1}{16}\omega^2} \qquad b_{28} = \frac{\frac{1}{4}a_6\omega Grc\lambda}{(n^2-n+M+k_p)^2+\frac{1}{16}\omega^2}$$

$$b_{29} = \frac{-\lambda a_7 Grc(n_3^2-n_3+M+k_p)}{(n_3^2-n_3+M+k_p)^2+\frac{1}{16}\omega^2} \qquad b_{30} = \frac{(\frac{1}{4}\lambda a_7 Grc\omega}{(n_3^2-n_3+M+k_p)^2+\frac{1}{16}\omega^2}$$

$$b_{31} = \frac{\lambda a_8 Grc\omega(n_4^2-n_4+M+k_p)}{(n_4^2-n_4+M+k_p)^2+\frac{1}{16}\omega^2} \qquad b_{32} = \frac{1}{4}\frac{\lambda a_8\omega Grc}{(n_4^2-n_4+M+k_p)^2+\frac{1}{16}\omega^2}$$

$$b_{33} = \frac{\lambda a_9 Grc(d_1^2+2d_1n_4-d_2^2+n_4^2-d_1-n_4+M+k_p)}{(d_1^2+2d_1n_4-d_2^2+n_4^2-d_1-n_4+M+k_p)^2+(2d_2(n_4+d_1)-d_2+\frac{1}{4}\omega)^2}$$

$$b_{34} = \frac{\lambda a_9 Grc(2d_2(n_4+d_1)-d_2+\frac{1}{4}\omega)}{(d_1^2+2d_1n_4-d_2^2+n_4^2-d_1-n_4+M+k_p)^2+(2d_2(n_4+d_1)-d_2+\frac{1}{4}\omega)^2}$$

$$b_{35} = \frac{\lambda a_{10} Grc(d_1^2+2d_1n_6-d_2^2+n_6^2-d_1-n_6+M+k_p)}{(d_1^2+2d_1n_6-d_2^2+n_6^2-d_1-n_6+M+k_p)^2+(2d_2(n_4+d_1)-d_2+\frac{1}{4}\omega)^2}$$

$$b_{36} = \frac{\lambda a_{10} Grc(2d_1d_2+2d_1n_6-d_2+\frac{1}{4}\omega)}{(d_1^2+2d_1n_6-d_2^2+n_6^2-d_1-n_6+M+k_p)^2+(2d_2(n_4+d_1)-d_2+\frac{1}{4}\omega)^2}$$

$$b_{37} = -\frac{\lambda a_{11} Grc(d_1^2+2d_1n_2-d_2^2+n_2^2-d_1-n_2+M+k_p)}{(d_1^2+2d_1n_6-d_2^2+n_6^2-d_1-n_6+M+k_p)^2+(2d_2(n_4+d_1)-d_2+\frac{1}{4}\omega)^2}$$

$$b_{38} = \frac{\lambda a_{11} Grc(2d_1d_2+2d_1n_2-d_2+\frac{1}{4}\omega)}{(d_1^2+2d_1n_6-d_2^2+n_6^2-d_1-n_6+M+k_p)^2+(2d_2(n_2+d_1)-d_2+\frac{1}{4}\omega)^2}$$

$$b_{39} = \frac{\lambda a_{12} Grc(n_5^2-n_5+M+k_p)}{(n_5^2-n_5+M+k_p)^2+\frac{1}{4}\omega^2} \qquad b_{40} = \frac{1}{4}\frac{\lambda a_{12} Grc\omega}{(n_5^2-n_5+M+k_p)^2+\frac{1}{4}\omega^2}$$

$$b_{41} = \frac{\omega^2}{(4M+4k_p)^2+\omega^2} \qquad b_{42} = \frac{\omega(4M+4k_p)}{(4M+4k_p)^2+\omega^2}$$

REFERENCES

[1] W. B. Hopper, T. S. Chen, and B. F. Armaly, *"Mixed convection along an isothermal vertical plate in porous medium with injection and suction"* , Numer Heat transfer Part A **25**, pp.317-329, 1994

[2] A. K. Singh, N. P. Singh, *Heat and Mass transfer in MHD flow of a viscous fluid past a vertical plate under oscillatory suction velocity*, Indian J. Pure Appl. Math., **34**(3), 429-442, 2003

[3] B. Sharma, M. Agarwal, R. C. Chaudhary, *MHD fluctuating free convective flow with radiation embedded in porous medium having variable permeability and heat source/sink*, J. Tech. Phys. **47**(1), 47-58, 2006.

[4] B. K. Sharma, R. C. Chaudhary, *Hydromagnetic unsteady mixed convection and mass transfer flow past a vertical porous plate immersed in a porous medium with Hall effect*, Eng. Trans. **56**(1), 3-23, 2008.

[5] B. K. Sharma, P. K. Sharma, R. C. Chaudhary, *Effects of fluctuating surface temperature and concentration on unsteady convection flow past an infinite vertical plate with constant suction*, Heat Transfer Research, **40** No 6, 505-519, 2009.

[6] G. Aaiza, I. Khan and S. Shafie, *Energy transfer in mixed convection unsteady magnetohydrodynamic (MHD) flow of an incompressible nanofluid inside a channel filled with saturated porous medium*, Nanoscale Research Letters, **10**:490-98, 2015. Springer open journals DOI 10.1186/s11671-015-1144-4.

[7] B. K. Sharma , T. Chand , R. C. Chaudhary , *"Hydromagnetic Unsteady Mixed Convection Flow Past an Infinite Vertical Porous Plate"*, Applied Mathematics, **1** No. 1, pp. 39-45, 2011. doi: 10.5923/j.am.20110101.05.

[8] S. Sebdani, M. Mahmoodi, S. Hashemi, *Effect of nanofluid variable properties on mixed convection in a square cavity*, Int J Therm Sci **52**,112–126, 2012

[9] T. Fan, H. XU, I. Pop, *Mixed convection heat transfer in horizontal channel filled with nanofluids*, International Journal of springer plus **34** 339–350, 2013.

[10] R. K. Tiwari, M. K. Das, *Heat transfer augmentation in a two-sided lid-driven differentially heated square cavity utilizing nanofluids*, Int J Heat Mass Transf **50** 9–10, 2007.

[11] G. A. Sheikhzadeh, N. Hajialigol, M. E. Qomi, A. Fattahi, *Laminar mixed convection of Cu-water nano-fluid in two sided lid-driven enclosures*, Journal of Nanostructures **1**44–53, 2012.

[12] K .A Maleque, *Unsteady Natural Convection Boundary Layer Flow with Mass Transfer and a Binary Chemical Reaction*, Hindawi Publishing Corporation, British Journal of Applied Science and Technology **3**(1): 131-149, 2013

[13] K .A Maleque, *A binary chemical reaction on unsteady free convective boundary layer heat and mass transfer flow with arrhenius activation energy and heat generation/absorption*, Latin American Applied Research **44**, 97-104.

[14] A. M. Okedoye, *Second Law Analysis of Mass Transfer Effect on Unsteady MHD flow Past an Accelerated Vertical Porous Plate*, International Journal of Pure and Applied mathematical Science and Technology **24**(2), 29 - 38, 2014.

[15] A. M. Okedoye, *Unsteady MHD mixed convection flow past an oscillating plate with heat source/sink*, Journal of Naval Architecture and Marine Engineering **11** 167-176., 11(1), 167 - 176, 2014. http://dx.doi.org//10.3329/jname.v11i2.6477.

[16] (O.D. Makinde, I.L. Animasaun. *Thermophoresis and Brownian motion effects on MHD bioconvection of nanofluid with nonlinear thermal radiation and quartic chemical reaction past an upper horizontal surface of a paraboloid of revolution*, Journal of Molecular Liquids **221** 733–743, 2016.

[17] O.D. Makinde, I.L. Animasaun. *Bioconvection in MHD nanofluid flow with nonlinear thermal radiation and quartic autocatalysis chemical reaction past an upper surface of a paraboloid of revolution*, International Journal of Thermal Sciences **109** 159-171, 2016.

[18] A. J. Chamkha, A. M. Rashad, H. Al-Mudhaf. *Heat and mass transfer from truncated cones with variable wall temperature and concentration in the presence of chemical reaction effects.* Int J Numer Meth Heat Fluid Flow; **22**,357–76, 2012.

[19] B. Mallikarjuna, A. M. Rashad, A. J. Chamkha, S. H. Raju. *Chemical reaction effects on MHD convective heat and mass transfer flow past a rotating vertical cone embedded in a variable porosity regime.* Afrika Matematika; **27**, 645–65, 2015.

[20] C. Zhang, L. Zheng, X. Zhang, G. Chen. *MHD flow and radiation heat transfer of nanofluids in porous media with variable surface heat flux and chemical reaction.* Appl Math Model; **39**:165–81, 2015.

[21] N. Khan, T. Mahmood, M. Sajid, M. S. Hashmi. *Heat and mass transfer on MHD mixed convection axisymmetric chemically reactive flow of Maxwell fluid driven by exothermal and isothermal stretching disks*, Int J Heat Mass Transf; **92**,1090–105, 2016.

[22] F. Mabood, S. Shateyi, M. M. Rashidi, E. Momoniat, N. Freidoonimehr. *MHD stagnation point flow heat and mass transfer of nanofluids in porous medium*

with radiation, viscous dissipation and chemical reaction, Adv. Powder Technol. **27**,742–9, 2016.

[23] S. Rawat, S. Kapoor, R. Bhargava. *MHD flow heat and mass transfer of micropolar fluid over a nonlinear stretching sheet with variable micro inertia density, heat flux and chemical reaction in a non-darcy porous medium*, J. Appl. Fluid Mech. **9**, 321–31, 2016.

[24] A. R. Bestman. *Natural convection boundary layer with suction and mass transfer in a porous medium*, Int J Eng Res; **14**, 389–96, 1990. http://dx.doi.org/10.1002/er.4440140403.

[25] O. D. Makinde, P. O. Olanrewaju, W. M. Charles. *Unsteady convection with chemical reaction and radiative heat transfer past a flat porous plate moving through a binary mixture*, Africka Matematika; **22**, 65–78, 2011.

[26] K. A. Maleque. *Effects of binary chemical reaction and activation energy on MHD boundary layer heat and mass transfer flow with viscous dissipation and heat generation/absorption*, ISRN Thermodyn **2013**, 9 pages, 2013.

[27] K. A. Maleque. *Effects of exothermic/endothermic chemical reactions with Arrhenius activation energy on MHD free convection and mass transfer flow in presence of thermal radiation*, J Thermodyn 2013. doi.org/10.1155/2013/692516.

[28] Z. Abbas and M. Sheikh and and S. S. Motsa, *Numerical solution of binary chemical reaction on stagnation point flow of Casson fluid over a stretching/shrinking sheet with thermal radiation*, Energy, **95**(C) 12-20, 2016.

[29] P. Resibois and M. De Leener, *The Mathematical Theory of the Kinetic Theory of Fluids* (Wiley, 1977).

[30] C. J. Van der Hoek, Contamination of a well in a uniform background flow, Report Dept. of Math., Agricult. Univ. Wageningen Technical Note pp. 90–03 (1990).

[31] S. O. Salawu and A. M. Okedoye. *Thermodynamic Second Law Analysis of Hydromagnetic Gravity-Driven Two-step Exothermic Chemical Reactive Flow with Heat Absorption Along a Channel*, Iranian Journal of Energy and Environment **9** (2): 114-120, 2018. doi: 10.5829/ijee.2018.09.02.0

[32] Z. G. Szabo, 1964, *Advances in kinetics of homogeneous gas reactions*, (Methusen and Co Ltd), Great Britain.

[33] O. D. Makinde, P. O. Olanrewaju, E. O. Titiloye, A. W. Ogunsola, *On thermal stability of a two-step exothermic chemical reaction in a slab*, Journal of Mathematical sciences. **13**, 1-15, 2013.

[34] Z. Shafique, M. Mustafa, A. Mushtaq. *Boundary layer flow of Maxwell fluid in rotating frame with binary chemical reaction and activation energy* Results in Physics **6** 627–633, 2016. journal homepage: www.journals.elsevier.com/results-in-physics

[35] O. D. Makinde, P. O. Olanrewaju, *Unsteady mixed convection with Soret and Dufour effects past a porous plate moving through a binary mixture of chemically reacting fluid*, Chemical Engineering Communications **198** 920–938, 2011.

[36] K. A. Maleque, *Effects of binary chemical reaction and activation energy on MHD boundary layer heat and mass transfer flow with viscous dissipation and heat generation/absorption*, Hindawi Publishing Corporation, ISRN Thermodynamics **2013**, 9pages. Article ID 284637,doi:10.1155/2013/284637.

[37] K. A. Maleque, *Unsteady natural convection boundary layer flow with mass transfer and a binary chemical reaction*, Hindawi Publishing Corporation, British Journal of Applied Science and Technology **2013**: 131–149, 2013.

[38] K. A. Maleque, *Effects of exothermic/endothermic chemical reactions with Arrhenius activation energy on MHD free convection and mass transfer flow in presence of thermal radiation*, Hindawi Publishing Corporation, Journal of Thermodynamics **2013**, Article ID 692516, doi:10.1155/2013/692516

[39] V. M. Soundalgekar and B .W. Martin and S. K. Gupta and I. Pop, *On Unsteady Boundary Layer in a Rotating Fluid with Time Dependent suction*, Publication De L'Institute Mathematique **20** 215-226, 1976.

[40] R. W. Bergstrom, *Viscous Boundary Layers in Rotating Fluids Driven by Periodic Flows*, Journal Atmospheric Science **33** 1234-1247, 1976.

[41] R. Nazar and N. Amin and I. Pop, *Unsteady boundary layer flow due to a stretching surface in a rotating fluid*, Mechanics Research Communications **31**:121-128, 2004.

[42] Z. Abbas and T. Javed and M. Sajid and N. Ali, *Unsteady MHD flow and heat transfer on a stretching sheet in a rotating fluid*, Journal of the Taiwan Institute of Chemical Engineers **41** 644-650, 2010.

[43] L. Zheng and C. Li and X. Zhang and Y. Gao, *Exact solutions for the unsteady rotating flows of a generalized Maxwell fluid with oscillating pressure gradient between coaxial cylinders*, Computers and Mathematics with Applications **62** 1105-1115, 2011.

[44] O .D. Makinde and P. O. Olanrewaju and W. M. Charles, *Unsteady convection with chemical reaction and radiative heat transfer past a flat porous plate moving through a binary mixture*, Africka Matematika **22** 65-78, 2011.

[45] O .D. Makinde and P. O. Olanrewaju, *Unsteady mixed convection with Soret and Dufour effects past a porous plate moving through a binary mixture of chemically reacting fluid*, Chemical Engineering Communications **198** 920-938, 2011.

[46] A. J. Chamkha and A. M. Rashad and H. Al-Mudhaf, *Heat and mass transfer from truncated cones with variable wall temperature and concentration in the presence of chemical reaction effects*, International Journal Numerical Meth Heat Fluid Flow 2012; **22** 357-76, 2012.

[47] A. M. Okedoye, *Second Law Analysis of Mass Transfer Effect on Unsteady MHD flow Past an Accelerated Vertical Porous Plate*, International Journal of Pure and Applied mathematical Science and Technology **24**(2), 29 - 38, 2014.

[48] Z. Shafique and M. Mustafa and A. Mushtaq, *Boundary layer flow of Maxwell fluid in rotating frame with binary chemical reaction and activation energy*, Results in Physics **6** 627-633, 2016.

[49] O. D. Makinde, P. O. Olanrewaju, and Charles, W.M. *Unsteady convection with chemical reaction and radiative heat transfer past a flat porous plate moving through a binary mixture*, Afri Mat. **22** 65-78, 2011. https://doi.org/10.1007/s13370-011-0008-z

[50] O. D. Makinde, N. Sandeep, T. M. Ajayi and I. L. Animasaun. *Numerical Exploration of Heat Transfer and Lorentz Force Effects on the Flow of MHD Casson Fluid over an Upper Horizontal Surface of a Thermally Stratified Melting Surface of a Paraboloid of Revolution*, International Journal of Nonlinear Sciences and Numerical Simulation, **19**, Issue 2, Pages 93–106, DOI: https://doi.org/10.1515/ijnsns-2016-0087

[51] O. D Makinde N, Sandeep, I. L. Animasaum and M. S Tshehla. *Numerical Exploration of Cattaneo-Christov Heat Flux and Mass Transfer in Magnetohydrodynamic flow over various geometries*, Defect and Diffusion Forum, **374**. 67-82. 2017. doi:10.4028/www.scientific.net/DDF374.67

[52] K. Avinash, N, Sandeep, O. D Makinde and I. L. Animasaum. *Aligned Magnetic Field Effect on radiative Biconvection flow past a vertical Plate with Thermophoresis and Brownian motion*, Defect and Diffusion Forum, **377**. pp 127-140. 2017. doi:10.4028/www.scientific.net/DDF377.127.

[53] Boddington T., Feng C. G. and Gray P., *Thermal explosions, criticality and the disappearance of criticality in systems with distributed temperatures I. Arbitrary Biot number and general reaction - rate laws*, Proc. R. Soc. Lond., 1983, A **390**, 247-264.

[54] Hammed Ogunseye and S. S. Okoya. Criticality and Thermal Explosion and the Flow of Reactive Viscous Third Grade Fluid Flow in a Cylindrical Pipe with Surface Cooling. Journal of the Nigerian Mathematical Society, **36**, Issue 2, pp. 399-418, 2017.

[55] Messhiha S.A.S. , *Laminar Boundary Layers in Oscillatory Flow along an Infinite Flat Plate with Variable suction*, Proc. Camb. Phil. Soc. **62** 329-337, 1966..

[56] M. J. Lighthill, *The response of laminar skin friction and heat transfer to fluctuations in the stream velocity*, Proceeding of the royal society of London **A224**, 1-23 1954.

DEPARTMENT OF MATHEMATICS AND COMPUTER SCIENCE, FEDERAL UNIVERSITY OF PETROLEUM RESOURCES, EFFURUN, DELTA STATE 334001, NIGERIA
E-mail address: okedoye.akindele@fupre.edu.ng

DEPARTMENT OF MATHEMATICS, COVENANT UNIVERSITY, CANAAN LAND, OTA, OGUN STATE, NIGERIA
E-mail addresses: peteroolmi@yahoo.com